

# Laser Welding of Fusion Relevant Steels for the European DEMO

Simon Kirk<sup>a</sup>, Wojciech Suder<sup>b</sup>, Keelan Keogh<sup>a</sup>, Tristan Tremethick<sup>a</sup>, Anthony Loving<sup>a</sup>

<sup>a</sup> United Kingdom Atomic Energy Authority, Culham Science Centre, Abingdon, OX14 3DB, UK

<sup>b</sup> Cranfield University, College Road, Cranfield, Bedfordshire, MK43 0AL, UK

The construction and maintenance of the European DEMO will require reliable joining of thick-walled Eurofer97 steel cooling pipes between in-vessel components in the reactor. To this end, laser welding has been investigated as a potential method for pipe joining. Two different techniques (keyhole laser welding and hybrid laser-laser welding) were used to produce test welds in Eurofer and P91 steel samples. Welds were also produced using different filler wires to reduce the hardness in the weldment region and improve the weld profile. Optical microscopy and hardness mapping were used to assess the quality of the welds produced. From the weld trials, suitable process parameters were identified that resulted in fully penetrated welds with good profiles. Here, we will present the results of the laser welding development process and the properties of the welds produced using these two techniques.

Keywords: DEMO, laser welding, service pipes, mechanical properties.

## 1. Introduction

The construction and maintenance of the European DEMO, and other large-scale fusion reactors, will require quick and reliable joining of cooling pipes between in-vessel components[1]. The joining process needs to be able to connect pipes with a wall thickness of 5 to 15 mm; the large thickness is due to the planned use of high pressure water and liquid metal coolants in the reactor. Due to the expected radiation level and limited access to pipework, the application of the joining process needs to be done using remote in-bore tools.

Laser welding has been selected for pipe joining as the process is fast, reliable, non-contact, results in a small heat affected zone and can weld thick sections in a single pass[2]. The joining process is required to produce fully-penetrated autogenous pipe welds with acceptable mechanical properties. Due to the space restrictions in the pipe, there can only be a small stand-off distance (approximately 10 mm) between the welding head and the material.

This work presented here is part of the EU Remote Maintenance programme. Alongside the welding trials described here, a prototype in-bore laser welding tool[3], with miniturised laser optics, has been developed to apply the welding process within a pipe.

## 2. Laser welding trials

A series of laser welding trials were performed on plate samples to identify suitable welding parameters and assess the quality of welds produced.

### 2.1 Materials

Laser welding trials were performed on 6 mm plate samples of Eurofer97[4], a reduced activation ferritic martensitic steel developed specifically for fusion environments, and P91[5], a carbon steel with analogous metallurgical properties to Eurofer97. Table 1 shows the composition of Eurofer97 and P91. Figure 1 shows the

time temperature transformation diagrams for Eurofer97 and P91; both steels can be seen to undergo the same microstructural changes. For both steels, the rapid post-weld cooling produces hard martensitic phases in the weldment which require post weld heat treatments to modify[5].

Table 1. Composition of Eurofer97[4] and P91[5] samples.

	Eurofer97	P91
<i>Fe</i>	bal.	bal.
<i>C</i>	0.1	0.1
<i>Cr</i>	9.0	9.0
<i>W</i>	1.0	-
<i>Mo</i>	-	1.0
<i>V</i>	0.2	-
<i>Ta</i>	0.1	-
<i>Y<sub>2</sub>O<sub>3</sub></i>	0.3	-
<i>Mn</i>	-	0.5
<i>Si</i>	-	0.3

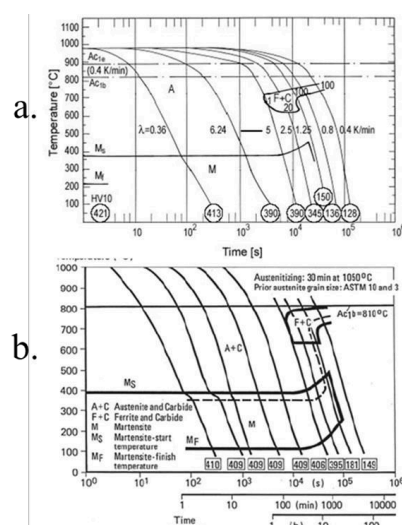


Fig. 1. Time temperature transformation diagrams for (a.) Eurofer97[4] and (b.) P91[5] steels.

Due to the scarcity of Eurofer97, the development of the welding process was done using P91 samples.

## 2.2 Welding process

Two different welding techniques were investigated for the joining process:

- Keyhole laser welding
- Laser-laser hybrid welding

Keyhole laser welding[2] uses a high power focused laser spot to generate a penetrating jet which melts the parent material. The keyhole region is driven along the joint to melt the parent materials which then cools and forms a solid welded region.

Laser-laser hybrid welding[7], shown schematically in figure 2, uses a defocused laser spot in tandem with a narrow-focused laser spot. The focused spot creates a keyhole welding region while the additional defocused laser provides pre/post-heating to modify the thermal history the material witnesses in the weld region, with the aim of producing beneficial microstructures. Laser-laser hybrid welding was trialed for the P91 and Eurofer joints to create a slower post-weld cooling rate and reduce the hardness of the weldment formed. Hybrid welding also improves the weld pool stability and can penetrate thicker materials compared with just keyhole welding.

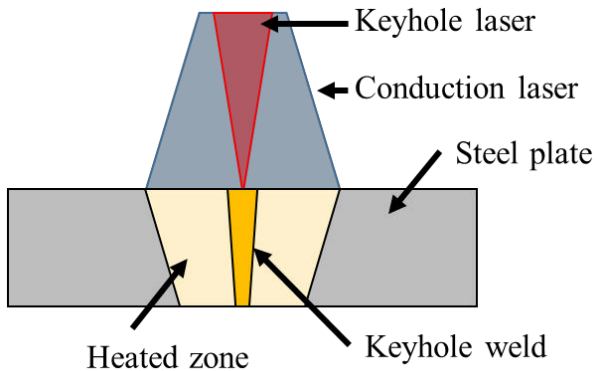


Fig. 2. Schematic of hybrid laser-laser welding.

The process parameters for each weld sample are listed in table 2.

## 2.3 Filler wire

Laser welds were also produced using filler wire to modify the local chemistry and reduce the hardness formed in the weldment region. Three filler wires were

trialed:

- Metrode 9CrMoV-N (AWS ER90S-B9, ER90S-B)
- Union NiMoCr (AWS A528-89, ER 100S-G)
- Lincoln Electric Supra MIG (AWS 8518)

The filler wires compositions are shown in table 3. Filler wires with reduced Carbon and Chromium contents were chosen to inhibit carbide formation. The filler wire samples were produced using hybrid laser welds in P91 plates (1 mm diameter wire, 2 m/min feeder speed).

Table 3. Filler wire compositions used in the welding trials. The P91 composition has been added for reference.

Material	Composition (wt.%)	P91 Steel	Metrode 9CrMoV-N	Union NiMoCr	Lincoln Supra MIG
		Fe	bal.	bal.	bal.
	C	0.1	0.1	0.08	0.08
	Cr	9.0	8.7	0.2	-
	Mo	1.0	-	0.5	-
	Ni	-	-	1.5	-
	Mn	0.5	0.5	1.7	1.7
	Si	0.3	0.25	0.6	0.85

## 3. Analysis of welds

The quality of the laser welds produced were assessed using optical microscopy and hardness mapping.

### 3.1 Optical microscopy

The Eurofer97 and P91 weld samples were sectioned, polished and etched using Nital solution to produce cross-section micrographs, shown in figure 3. The weldment, Heat Affected Zone (HAZ) and parent material regions can be clearly seen in all four welds. The weldment region has a coarse grain structure compared to the surrounding regions in all the welds. The weldment regions have an hour-glass shape with the hybrid welds (B) having a wider top where the additional heat input caused greater melting. All the welds are fully penetrated, with a good root, and show no porosity or cracking. The keyhole welds (A & C) have a good convex cap on top of the weld. But the hybrid welds (B & D) are undercut at the top. The weld profiles are identical in both Eurofer97 and P91.

Table 2. Weld sample process parameters.

Weld	Material	Process	Weld speed (mm/s)	Keyhole laser power (kW)	Keyhole spot diameter (mm)	Conduction laser power (kW)	Conduction spot diameter (mm)
A	P91	Keyhole	0.5	4	0.6	-	-
B	P91	Hybrid	0.5	3	0.2	5	8
C	Eurofer97	Keyhole	0.5	4	0.6	-	-
D	Eurofer97	Hybrid	0.5	3	0.2	5	8

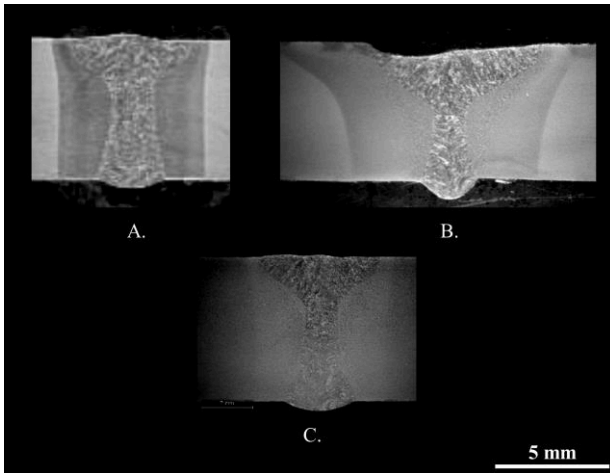


Fig. 3. Cross-section micrographs of the laser weld samples: (A.) P91 Keyhole, (B.) P91 Hybrid and (C.) Eurofer97 Keyhole.

### 3.2 Hardness mapping

Hardness mapping was used to assess the phases formed and resulting mechanical properties in the weld regions. The welds were mapped by measuring hardness across a grid of points (1.0 mm spacing) using a LECO AMH43 microindenter with a 100  $\mu\text{m}$  pyramid indenter and 100 g indentation load. The base hardness of the parent Eurofer97 and P91 materials were  $240 \pm 10$  HV and  $220 \pm 5$  HV, respectively.

Figure 4 shows the hardness maps measured for the weld samples. The hardness in the weldment and HAZ are significantly higher than the parent material in all the welds. Comparing the hardness maps and the micrographs, in figure 3, the edge of the high hardness region lines up with the HAZ-parent material boundary. The hardness is uniformly high across the weldment and HAZ, and there is a sharp change between the HAZ and parent material. Also the hardness is uniform despite the large difference in grain sizes between the HAZ and weldments.

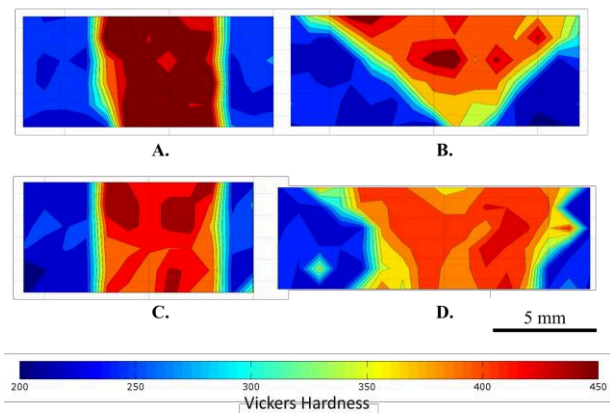


Fig. 4. Hardness maps of the weld samples: (A.) P91 Keyhole, (B.) P91 Hybrid, (C.) Eurofer97 Keyhole and (D.) Eurofer97 Hybrid.

The hybrid welds (B & D) had similar peak hardness,  $450 \pm 10$  HV, as the keyhole welds (A & C) despite the reduced cooling durations. The high hardness regions are wider in the hybrid welds, but mirror the shape of the weld regions observed in the micrographs.

The shape of hardness maps are the same in the P91 and Eurofer97 welds for both processes, as seen in the micrographs.

### 3.3 Filler wire welds

The filler wire welds were assessed using chemical and hardness measurements. Figure 5 shows the hardness distribution across the centerline of the welds produced using the different filler wires. Despite the difference in chemical composition, no significant reduction in hardness was produced by any of the filler wires in comparison of with the P91, no filler, welds.

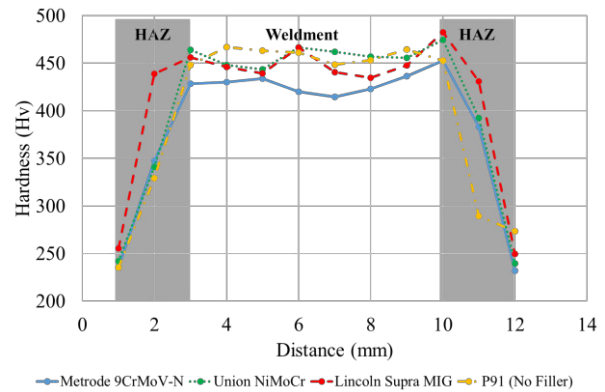


Fig. 5. Hardness distribution across the P91 filler wire welds.

Energy-Dispersive X-ray spectroscopy (EDX)[8] was used to measure the chemical composition in the parent metal, HAZ and weldment regions to assess the effectiveness of the chemical modification. Table 4 shows the chemical content distribution for filler wire welds. Despite the significant difference in filler wire and parent material compositions, only minor chemical modifications ( $\sim 1\%$  reduction in Cr content) was seen in the weldment region. No changes were seen in the HAZ for any of the filler wire welds.

Table 3. EDX measured chemical contents of the parent, HAZ and weldment regions of the filler wire welds.

Filler Wire	Weld Region	Chemical content (wt.%)		
		Cr	Fe	Mo
Metrode 9CrMoV-N	Parent	9.68	88.97	0.85
	HAZ	9.88	89.39	0.85
	Weldment	8.50	91.68	0.72
Union NiMoCr	Parent	9.61	88.95	0.80
	HAZ	9.68	98.54	0.70
	Weldment	8.62	96.69	0.71
Lincoln Supra MIG	Parent	9.52	89.02	0.72
	HAZ	9.60	88.65	0.73
	Weldment	8.75	90.11	0.69

## 5. Discussion

Keyhole and hybrid laser-laser welds were produced in both Eurofer97 and P91 steel plates. The acceptance requirements for the weld are:

- Full penetration
- No cracking or large-scale porosity
- A positive, convex, cap at the top
- A positive root at the base
- Uniform hardness across the weld

The keyhole welding process produced fully penetrated welds with no cracking or porosity, and acceptable caps and roots in both materials. However the hardness was unacceptably high in the weldment and HAZ compared with the parent material.

The hybrid laser-laser process produced fully penetrated welds with no cracking or porosity and a good root, but there was some undercutting at the surface which can act as an initiation point for failure. Like the keyhole process, the hybrid welds had identical profiles in both materials which is due to their near identical thermal properties[4,5] (melting point, thermal conductivity, etc.). Again, the hardness in the weldment and HAZ are unacceptably high.

Comparing the hardness and microscopy results, the high hardness regions include the weldments and HAZs in all the weld. The hardness is also uniform across these regions despite the visible difference in grain size. These results indicate the high hardness is caused by a hard martensitic phase[4,5] forming in the weldment and HAZ. The high hardness region is likely to have reduced ductility and fatigue strength compared with the parent material[5]. The steep change in mechanical properties at the phase change boundary between the HAZ and parent material could act as an initiation site for crack growth due to residual stresses[9].

The attempt to modify the weld chemistry using filler wires failed to reduce the hardness in the weld region. The lack of change was attributed to insufficient diffusion time and mixing in the weld. This meant the chemical depletion remained in the deposited material at the top of the weld and did not penetrate into the bulk of the weld, as observed in the chemical measurements.

As the high hardness region was not reduced by chemical modification or slower cooling in the hybrid process, a post-weld heat treatment is required[6]. If laser welding is to be used in DEMO remote maintenance schemes then tooling will be required to apply a post-weld heat treatment process at the weld site.

Undercutting in the hybrid welds could be solved by providing additional filler material to the weld. In conventional welding these would be achieved with filler wire, however in remote welding supplying a filler wire is unfeasible. Additional material can be provided to a remote weld by including an overhanging feature in the pipe end profile[2].

## 6. Conclusions

As part of developing remote in-bore welding tools for the European DEMO, a series of Eurofer97 and P91 6mm plate welds were produced using keyhole laser welding and hybrid laser-laser welding. The conclusions from these trials were as follows:

- Optical microscopy showed the welds were fully penetrated.
- The keyhole welds had good profiles, but the hybrid laser welds were undercut due to a lack of material in autogenous welds.
- The welds had high hardness in the weldment and HAZ due to the formation of martensite phases.
- Attempts to modify the weld chemistry using filler wires had no effect on the weld hardness.
- The welding processes resulted in identical welding profiles in both Eurofer97 and P91, due to their similar thermal properties.
- The Eurofer97 and P91 samples were found to have similar weld hardnesses.
- The results demonstrated that P91 is a suitable simulant material for Eurofer97 in welding trials.
- Post-weld heat treatment will be required for the laser welds.

Future work on this project will be aimed at reproducing these welding processes using a remote in-bore prototype tool.

## References

- [1] O. Crofts et al., Overview of progress on the European DEMO remote maintenance strategy, *Fusion Engineering and Design* 109 (2016) 1392-1398.
- [2] J. Ion, *Laser processing of engineering materials: principles, procedure and industrial application*. Butterworth-Heinemann, Oxford, 2005.
- [3] K. Keogh et al., *Laser Cutting and Welding Tools for use In-bore on EU DEMO Service Pipes*, *Fusion Engineering and Design* (2017), in preparation.
- [4] R. Lindau et al., Present development status of EUROFER and ODS-EUROFER for application in blanket concepts, *Fusion Engineering and Design* 75 (2005) 989-996.
- [5] V.T. Paul, S. Saroja, & M. Vijayalakshmi, Microstructural stability of modified 9Cr-1Mo steel during long term exposures at elevated temperatures, *Journal of Nuclear Materials* 378 (3) (2008) 273-281.
- [6] M. Rieth & J. Rey, Specific welds for test blanket modules, *Journal of Nuclear Materials* 386 (2009) 471-474.
- [7] W. Suder et al., Comparison of joining efficiency and residual stresses in laser and laser hybrid welding, *Science and Technology of Welding and Joining* 16(3) (2011) 244-248.

- [8] J. Goldstein et al. Scanning electron microscopy and X-ray microanalysis: a text for biologists, materials scientists, and geologists. Springer Science & Business Media, Berlin, 2012.
- [9] K. Masubucki, Analysis of welded structures: residual stresses, distortion, and their consequences. Elsevier, Oxford, 2013

## **Acknowledgements**

The Authors would like to thank Dr. Supriyo Ganguly, Cranfield University, for his advice on this work and Dr. Mike Gorley, UKAEA, for providing Eurofer97 material samples.

This work has been carried out within the framework of the EUROfusion Consortium and has received funding from the Euratom research and training programme 2014-2018 under grant agreement No 633053. The views and opinions expressed herein do not necessarily reflect those of the European Commission.

2018-03-30

# Laser welding of fusion relevant steels for the European DEMO

Kirk, Simon

Elsevier

---

Kirk S, Suder W, Keogh K, et al., (2018) Laser welding of fusion relevant steels for the European DEMO. Fusion Engineering and Design, Volume 136, Part A, November 2018, pp. 612-616  
<https://doi.org/10.1016/j.fusengdes.2018.03.039>

*Downloaded from Cranfield Library Services E-Repository*